1 Basic Physics

We will begin our study of fusion plasmas by considering the basic physics that ultimately determines the properties of a thermonuclear plasma. The fusion process will be considered in the first section, and the conditions necessary for the achievement of fusion reactions will be established. In the second section, we will examine some fundamental properties of a plasma and will establish the criterion that determines when a collection of charged particles may be treated as a plasma. The consequences of charged-particle (Coulomb) collisions upon the particles that make up a plasma will be examined in the third section. Finally, the basic equations of electromagnetic theory will be reviewed in the fourth section.

1.1 Fusion

The actual mass of an atomic nucleus is not the sum of the masses (m_p) of the Z-protons and the masses (m_n) of the A–Z neutrons of which it is composed. The stable nuclides have a mass defect

$$\Delta = [Zm_p + (A–Z)m_n] - Am_z \tag{1.1}$$

This mass defect is conceptually thought of as having been converted to energy ($E = \Delta c^2$) at the time that the nucleus was formed, putting the nucleus into a negative energy state. The amount of externally supplied energy that would have to be converted to mass in disassembling a nucleus into its separate nucleons is known as the "binding energy" of the nucleus, BE $= \Delta c^2$. The binding energy per nucleon (BE/A) is shown in Fig. 1.1.

Any process which results in nuclides being converted to other nuclides with more binding energy per nucleon will result in the conversion of mass into energy. The combination of low A-nuclides to form higher A-nuclides with a larger BE/A is the basis for the fusion process for the release of nuclear energy. The splitting of very high A-nuclides to form intermediate A-nuclides with a larger BE/A is the basis of the fission process for the release of nuclear energy.

The fusion of two light nuclei to form a compound nucleus in an excited state that then decays into reaction products, with an attendant conversion of mass into kinetic energy, is represented schematically by

$$a + b \rightarrow \begin{pmatrix}\text{compound}\\ \text{nucleus}\end{pmatrix}^* \rightarrow c + d \tag{1.2}$$

The mass difference

$$\Delta m = (m_a + m_b) - (m_c + m_d) > 0 \tag{1.3}$$

Fusion Plasma Physics. Weston M. Stacey

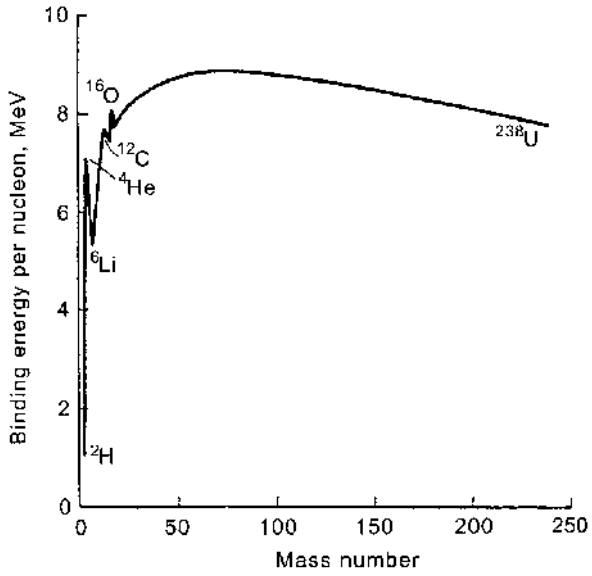

Figure 1.1. Binding energy per nucleon

is converted into kinetic energy according to Einstein's celebrated formula

$$\Delta E = (\Delta m)c^2 \tag{1.4}$$

In order for the fusion reaction to take place, the two nuclei must overcome the long-range Coulomb repulsion force and approach sufficiently close that the short-range nuclear attraction forces can lead to the formation of a compound nucleus. From the observation that hydrogen, deuterium, helium, and so on, do not fuse spontaneously under normal conditions, we conclude that the electrostatic repulsion between positively charged nuclei prevents nuclei approaching each other sufficiently close for the short-range attractive nuclear forces to become dominant. For fusion to occur as a result of random encounters between atomic nuclei, the nuclei must be made sufficiently energetic to overcome the Coulomb repulsive force. We will see that energies of the order of 10 keV to 100 keV are required, which corresponds to temperatures of 10^8 K to 10^9 K. At these thermonuclear temperatures, which are comparable to those of the sun's interior, light atoms are completely stripped of their orbital electrons. This macroscopically neutral gas of positively charged light atomic nuclei and electrons is a thermonuclear plasma.

The rate at which fusion reactions take place between atomic nuclei of species 1 and 2 in a thermonuclear plasma is

$$n_1 n_2 \langle \sigma \upsilon \rangle_f \equiv n_1 n_2 \int_{\upsilon_1 \upsilon_2} f_1(\upsilon_1) f_2(\upsilon_2) |\upsilon_1 - \upsilon_2| \sigma_f(|\upsilon_1 - \upsilon_2|) \, \mathrm{d}^3\upsilon_1 \, \mathrm{d}^3\upsilon_2 \tag{1.5}$$

where n_1 is the density, υ_1 is the velocity, and f_1 is the velocity distribution function, respectively, of species 1, and σ_f is the fusion cross section. The velocity distributions of

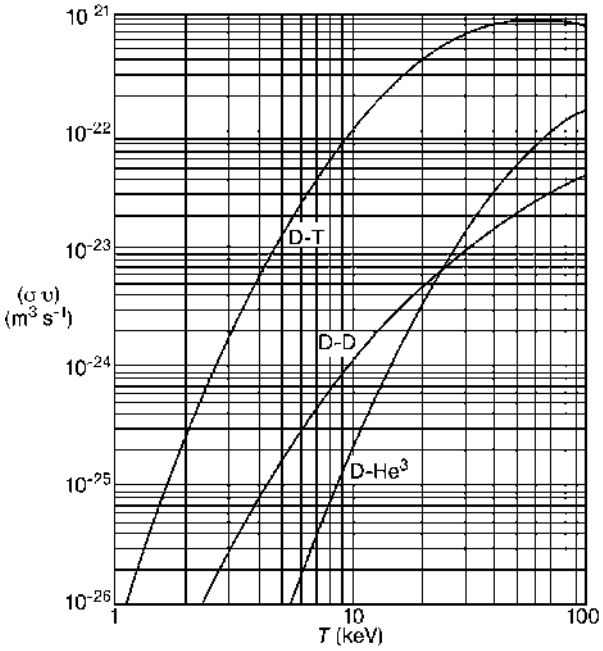

Figure 1.2. Fusion reaction rates

ions in a plasma can be represented in many cases by a Maxwellian distribution

$$f_{\max} = \left(\frac{m_{\mathrm{i}}}{2\pi T_{\mathrm{i}}}\right)^{\frac{3}{2}} e^{-(m_{\mathrm{i}}\upsilon^2)/2T_{\mathrm{i}}} \tag{1.6}$$

where T_i and m_i are the temperature and mass, respectively, and k is the Boltzmann constant. We will see that Coulomb collisions will cause all light ion species in a plasma to have about the same velocity distribution, so that the parameter $\langle \sigma \upsilon \rangle_f$ in Eq. (1.5) can be evaluated as a function of a single temperature $T = T_1 = T_2$.

Fusion reaction rates for the three reactions of primary interest for thermonuclear plasmas are shown in Fig. 1.2. At temperatures below the threshold value shown in Fig. 1.2 the reaction rates are negligible. As is apparent from this figure, and from Table 1.1, the reaction rate which becomes significant at the lowest temperature is for deuterium (D)–tritium (T) fusion. Table 1.1 also gives the amount of thermonuclear energy produced by a fusion event and indicates the part of that energy that is the kinetic energy of a neutron. The two branches shown for the D–D reaction occur with about equal probability. There are many other possible fusion reactions, but they generally have even higher threshold energies.

We can identify the principal challenges of fusion research from these data. The plasma must be heated to thermonuclear temperature (10^8 K to 10^9 K) and confined sufficiently long that the thermonuclear energy produced significantly exceeds the energy required to

Table 1.1. Fusion reactions of primary interest

Reaction	Thermonuclear energy release MeV	Threshold energy K	keV
$D + T \rightarrow {}^4He + n\ (14.1\,MeV)$	17.6	4.5×10^7	4
$D + D \rightarrow \begin{cases} T + p \\ {}^3He + n\ (2.5\,MeV) \end{cases}$	4.0 3.25	4.0×10^8	35
$D + {}^3He \rightarrow {}^4He + p$	18.2	3.5×10^8	30

heat the plasma. A simple energy balance (which ignores many important effects),

$$\left(\tfrac{1}{4}n^2\langle\sigma\upsilon\rangle_f E_f\right)\tau_E > 3nT \tag{1.7}$$

which states that the product of the fusion energy production rate and the energy confinement time, τ_E, must exceed the amount of energy required to heat n ions per unit volume ($n_1 = n_2 = \frac{1}{2}n$) and n electrons to temperature T, may be used to derive a break-even criterion for the scientific feasibility of fusion power. Using physical constants typical of a D–T plasma, Eq. (1.7) can be rearranged to write the criterion

$$nT\tau_E > \frac{12k}{\dfrac{\langle\sigma\upsilon\rangle_f}{T^2}}E_f \simeq 3 \times 10^{21}\,\mathrm{keV}\cdot\mathrm{s}^{-1}\mathrm{m}^{-3} \tag{1.8}$$

The quantity $\frac{\langle\sigma v\rangle_f}{T^2}$ is approximately constant around 10 keV for the D–T reaction.

No conceivable material could confine a plasma at thermonuclear temperatures. Plasmas at these temperatures coming into direct contact with a material wall would produce wall vaporization, which would quickly destroy the wall and quench plasma due to the radiation produced by the ions of the wall material in the plasma. Thus, means other than wall confinement are necessary.

Two basically different approaches to achieving energy break-even are being pursued. In the first approach, use is made of the fact that charged particles spiral about magnetic field lines to create magnetic field configurations which confine plasmas in a magnetic trap. The goals of magnetic confinement research are to achieve plasma densities of $\sim 10^{20}\,\mathrm{m}^{-3}$ to $10^{22}\,\mathrm{m}^{-3}$ and energy confinement times of $\sim 10^{-1}$ s to 10^1 s. Magnetically confined plasmas are to be heated to thermonuclear temperatures by a number of different possible means.

In the second approach, known as inertial confinement, a 1 mm to 10 mm D–T pellet is compressed to densities of $10^{27}\,\mathrm{m}^{-3}$ to $10^{28}\,\mathrm{m}^{-3}$ and heated to thermonuclear temperatures by lasers or fast ion beams. In the 10 ns to 100 ns required for explosive disassembly, fusion takes place at a prodigious rate.

Progress in achieving the plasma conditions needed for fusion power is shown in Fig. 1.3, where the product of the central plasma density and the energy confinement time are plotted on the vertical axis versus the plasma temperature. The plasma conditions achieved in several generations of the leading tokamak confinement system experiments since 1958 have increased dramatically towards the conditions needed for a fusion

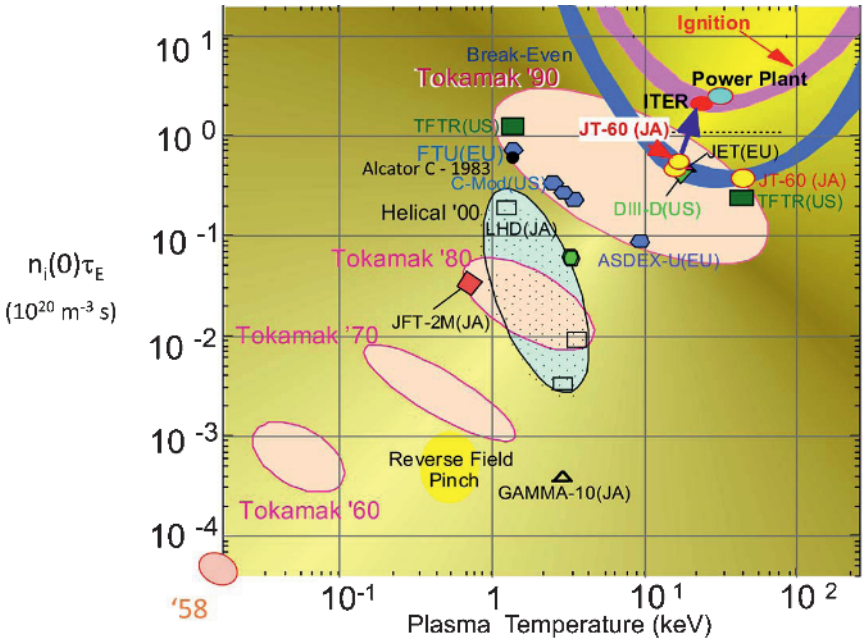

Figure 1.3. Progress in Magnetic Confinement Plasma Physics

power plant. Also shown are the parameters achieved in several other magnetic confinement configurations–stellarators (helical), reversed field pinch and the Gamma-10 mirror experiment. Clearly, the temperatures required for fusion power have been achieved and only small further advances in energy confinement are needed. The ITER tokamak experimental power reactor, presently under construction to operate in the 2020s, should achieve the plasma temperature and confinement on the threshold of values required for a power reactor.

Fusion is being developed as an energy source. By the year 2050 the world's electricity usage is estimated to require 0.42×10^{21} Joules/yr annual fuel consumption. At this rate of consumption: i) the world's proven reserves of fossil fuels would be exhausted in less than a century, even if their environmental impact did not prohibit their use earlier; ii) the world's proven reserves of uranium would be exhausted in about 4 years with the present "once-through" fuel cycle that only extracts less than 1 % of the energy; and iii) even if "breeder" reactors are implemented to recover a much greater fraction of the uranium energy potential, by converting the "fertile" uranium and thorium resources to "fissionable" plutonium and uranium, this resource would be exhausted in less than a century. None of these fuels will provide all of the electrical energy in 2050, of course, but dividing these numbers by the fraction that they may provide gives some perspective as to their limitation as future fuel supplies.

On the other hand, the world's proven lithium reserves are capable of producing enough tritium to enable D-T fusion to meet the 2050 rate of consumption for several thousand years. The fuel supply for D-D fusion (1 in every 10,000 water molecules contains a deu-

terium atom) is virtually infinite. Thus, fusion will inevitably be the ultimate energy source of mankind, and it will need to be making significant contributions by the end of the present century if we are to maintain our standard of life and extend it to others less fortunate.

The theoretical treatment of plasma physics is based on the electromagnetic relations of Maxwell, the laws of motion of Newton under the force laws of Coulomb and Lorentz, and the statistical theory of gases of Maxwell and Boltzmann, with very few exceptions in which quantum mechanics or relativity physics are needed. However, a thermonuclear plasma of the type addressed in this book consists of on the order of 10^{20} charged particles per cubic meter moving in response to their mutual electromagnetic interactions and the forces exerted by external electromagnets. Such a collection of charged particles is an inherently collective state of matter, so the problem of magnetic fusion plasma physics is one of immense complexity.

In order to represent mathematically and calculate simultaneously the motion of on the order of 10^{20-22} mutually interacting charged particles moving in externally applied magnetic and (sometimes) electric fields is a formidable computational challenge. Although advances in digital computer technology have enabled some progress to be made recently with direct, "brute-force" calculations (that include only relatively few approximations) of limited subsets of this quantity of electromagnetically interacting charged particles, the major progress in magnetic fusion plasma physics theoretical understanding has resulted from using physical insight to develop computationally tractable mathematical representations of the physics. These approximate theoretical models then can be compared with experimental measurements, refined to improve the agreement, and used to guide the design of the next experiments, which will (hopefully) achieve better performance parameters but will surely guide the development of theoretical understanding by exposing new phenomena that must be explained. As illustrated in Fig. 1.3, this has been a remarkably successful enterprise.

Perhaps the boldest of the mathematical representations of fusion plasma physics is the single particle model in which it is assumed that the motion of a single "test particle" can be calculated by: i) representing the electromagnetic forces due to most of the vast number of other charged particles in the plasma (and in external electromagnets) as known electromagnetic forces acting on the single test particle due to the magnetic and electric fields produced by these other particles; but ii) treating the simultaneous interactions of the test particle with the large number of extremely nearby particles whose Coulomb attractive or repulsive forces can be distinguished as a sum of two-body electrostatic interactions with each of the multitude of such nearby particles.

In the following sections, we first motivate this approximation by consideration of the extremely short-range attenuation of the electrostatic potential due to a given charged particle by the presence of other nearby charged particles. Then a 'scattering" formalism is developed for treating the short-range interactions under the Coulomb force acting between two particles in order to derive an effective collective force due to Coulomb scattering with extremely nearby particles. Finally the calculation of electric and magnetic fields produced by the distribution and motion of more distant charged particles and the resultant electromagnetic forces are reviewed. Once these forces are established, the motion of a single charged particle can be determined by solving Newton's law of motion

$F = ma$. This simple picture of a plasma naturally works best in situations in which the external magnetic fields are much greater than those produced by the plasma particles. It will enable an investigation of particle motion in various magnetic field configurations and the identification of likely magnetic confinement systems.

More sophisticated treatments of collective effects – the kinetic theory of the distribution functions of mutually interacting particle species and fluid theories for the density and pressure of these plasma species – will subsequently be developed and employed, together with the equations of electromagnetics, to investigate a rich variety of plasma phenomena. The mathematical development will be related to experimental results, particular in those areas that are still the subject of active research.

1.2 Plasma

A plasma is a collection of charged particles which is macroscopically neutral over a volume that is small compared to its dimensions. In principle, the motion of each particle can be determined from Newton's second Law and the electrostatic force that each particle exerts on all other particles. This is impractical in practice, because there might be some 10^{20} particles in a cubic meter of magnetically confined plasma, so other means of describing the plasma must be found. The fact that the electrostatic potential $\phi = e/(4\pi\epsilon_0 r)$ that a particle of charge e produces at a distance r is shielded by the presence of nearby charged particles can be exploited to develop a computationally tractable approximation.

Although a plasma is macroscopically neutral, it is locally nonneutral on some sufficiently small microscopic scale. Consider a macroscopically neutral plasma with a uniform ion distribution of density n_0 and a locally nonuniform electron distribution which varies according to the Maxwell–Boltzmann distribution

$$n_e = n_0 \exp\left(\frac{e\phi}{T_e}\right) \approx n_0 \left(1 + \frac{e\phi}{T_e}\right) \tag{1.9}$$

where $|e\phi| \ll |T_e|$. The local electrostatic potential, ϕ, arises from local nonuniformities in the electron distribution which lead to a local charge density $e(n_i - n_e) = e(n_0 - n_e)$. The potential satisfies Poisson's equation

$$\nabla^2\phi = \frac{e(n_e - n_0)}{\epsilon_0} = \frac{1}{\lambda_e^2}\phi \tag{1.10}$$

where we have used Eq. (1.9) in the last step and defined the electron Debye length

$$\lambda_e \equiv \left(\frac{\epsilon_0 T_e}{n_0 e^2}\right)^{\frac{1}{2}} \tag{1.11}$$

We know that the solution of Poisson's equation for an isolated point charge is $e/(4\pi\epsilon_0 r)$. Accordingly, we search for a solution to Eq. (1.10) which approaches this form as $r \to 0$ and which vanishes as $r \to \infty$. The appropriate solution, satisfying these boundary conditions, is

$$\phi(r) = \frac{e}{4\pi\epsilon_0 r} \exp\left(-\frac{r}{\lambda_e}\right) \tag{1.12}$$

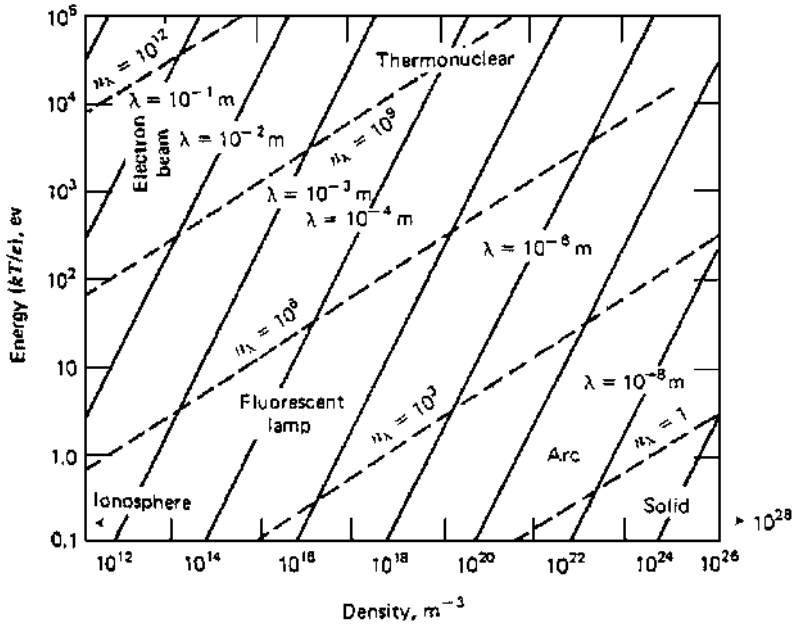

Figure 1.4. Debye length and number of particles in a Debye sphere

Equation (1.12) describes a Coulomb potential at small r, ($r \ll \lambda_e$) but decreases much more rapidly than a Coulomb potential for $r \gtrsim \lambda_e$. Thus, the electrostatic potential arising from a microscopic nonuniformity in density – for example, the location of a charged particle – is shielded by a cloud of other charged particles within a distance λ_e. In order for this argument to be valid, the number of particles inside a sphere of radius λ_e must be large

$$n_\lambda \equiv \tfrac{4}{3}\pi\lambda_e^3 n_0 = \tfrac{4}{3}\pi\left(\frac{\epsilon_0 T_e}{n_0 e^2}\right)^{\frac{3}{2}} n_0 \gg 1 \tag{1.13}$$

(Note that the Debye length is the same for singly charged ions and electrons at the same temperature.) Equation (1.13) defines the criterion that must be satisfied in order for the collection of charged particles to be a plasma. As can be seen from Fig. 1.4, plasmas exist over a wide range of densities (including solids) and temperatures.

In plasmas for which condition (1.13) is satisfied, the forces acting on a charged particle may be separated into two types for the purpose of developing a tractable computation approximation. The interaction of a given charged test particle with all other charged particles separated from it by λ_e or more may be treated by calculating the electric and magnetic fields produced by these other particles at the position of the test particle and the associated forces. The interactions of the test particle with all charged particles within less than λ_e of the test particle may be treated as two-body scattering interactions governed by the Coulomb electrostatic force acting between the two particles. The unshielded Coulomb potential $\phi = e/4\pi\epsilon_0 r$ is used in the latter calculation. Thus, the equation of motion of

the test particle may be written

$$m\left(\frac{\mathrm{d}\boldsymbol{v}}{\mathrm{d}t}\right) = e(\boldsymbol{E} + \boldsymbol{v} \times \boldsymbol{B}) + \boldsymbol{F}_{\mathrm{sc}} \tag{1.14}$$

where $\boldsymbol{E}$ and $\boldsymbol{B}$ are the electric and magnetic fields caused by other charges and currents due to the plasma particles and to external sources, and $\boldsymbol{F}_{\mathrm{sc}}$ is the force on the test particle due to the two-body scattering interactions with the other particles within λ_e of it.

The Debye length prescribes a lower limit on the macroscopic dimensions (L) of a plasma, by definition. For $L \leq \lambda_{\mathrm{e}}$, the medium would behave as a collection of free charges dominated by mutual two-body interactions. For plasmas of thermonuclear interest, $\lambda_{\mathrm{e}} \approx 10^{-5}$ m to 10^{-3} m, $N_\lambda \gg 1$, and $L \sim 1$ m.

A considerable amount can be learned about plasmas and their confinement by investigating the consequences of Eq. (1.14). First, it is necessary to calculate $\boldsymbol{E}$, $\boldsymbol{B}$ and $\boldsymbol{F}_{\mathrm{sc}}$, which is the purpose of the next two sections.

As an example of the collective treatment of a plasma, which also introduces the important concept of plasma frequency, consider a uniform plasma slab. Assume that at $t = 0$ all the electrons in the interval $x_1 < x < x_0$ are displaced to the left of x_1, as shown in Fig. 1.5. Further assume that the ions are fixed. The excess charge to the left of x_1, is $-n_0 e(x_0 - x_1)$. From Gauss' law, this produces a field at x_1, in the $-x$–direction of magnitude

$$E(x_1) = \frac{n_0 e}{\epsilon_0}(x_0 - x_1)$$

This field exerts a force on the electrons at x_1, the equation of motion for which is

$$m_{\mathrm{e}}\ddot{x}_1 = eE(x_1) = \frac{e^2 n_0}{\epsilon_0}(x_0 - x_1) \tag{1.15}$$

In terms of the relative displacement,

$$\xi \equiv x_0 - x_1 \tag{1.16}$$

this equation may be written

$$\frac{\mathrm{d}^2\xi}{\mathrm{d}t^2} + \left(\frac{e^2 n_0}{m_{\mathrm{e}}\epsilon_0}\right)\xi = 0 \tag{1.17}$$

This is the harmonic oscillator equation, with solution

$$\xi\,(t) = \mathrm{A}e^{i\omega_{\mathrm{pe}}t} + \mathrm{B}e^{-i\omega_{\mathrm{pe}}t} \tag{1.18}$$

where

$$\omega_{\mathrm{pe}} \equiv \left(\frac{e^2 n_0}{m_{\mathrm{e}}\epsilon_0}\right)^{\frac{1}{2}} \tag{1.19}$$

is the electron *plasma frequency*. A similar definition for the ion plasma frequency is

$$\omega_{\mathrm{pi}} \equiv \left(\frac{z^2 e^2 n_0}{m_{\mathrm{i}}\epsilon_0}\right)^{\frac{1}{2}} \tag{1.20}$$

where z is the ion charge.

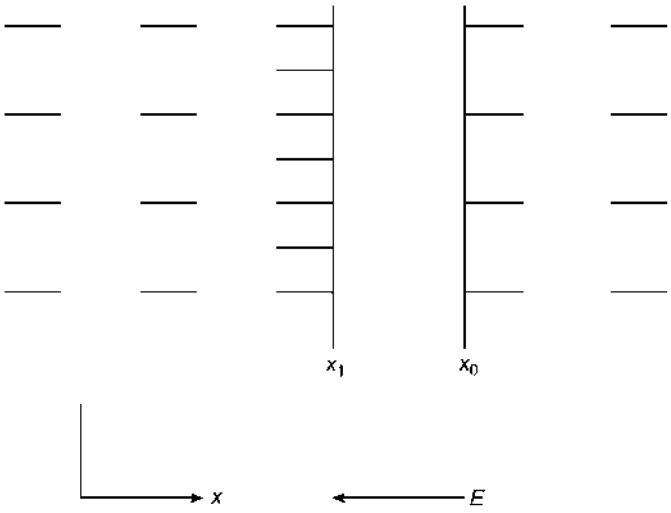

Figure 1.5. Plasma slab at $t = 0$

Thus we see that the plasma frequency is a natural frequency of oscillation for each species in the plasma. As is well known from the theory of harmonic oscillators, the oscillations can be excited in response to an external stimulus with frequency less than or equal to the natural frequency. Thus each plasma species can respond to an internal perturbation with frequency $\omega < \omega_p$. Because

$$\omega_{pi} = z\sqrt{\frac{m_e}{m_i}}\omega_{pe} \tag{1.21}$$

electrons are able to respond to much higher frequency perturbations than are ions. In MKS units, Eq. (1.19) is

$$\omega_{pe} = 56.4\sqrt{n_0}\,\text{rad/s} \tag{1.22}$$

so that for a typical thermonuclear plasma density of $n_0 \approx 10^{20}\,\text{m}^{-3}$, $\omega_{pe} \approx 5{\times}10^{11}$ rad/s.

1.3 Coulomb Collisions

Although most electrostatic interactions among particles in a plasma take place over distances that are large compared to a Debye length and can be treated collectively by fields, a smaller number of interactions take place over distances comparable to or less than a Debye length. These interactions, although relatively few in number, have important effects upon the properties of a plasma. These close encounters are treated separately, as scattering events, and take place on a time scale that is very short compared to most other plasma phenomena so that they may be considered to take place instantaneously.

The geometry of the scattering process is illustrated in Fig. 1.6. A particle of mass m_1 and initial velocity v_1, approaches a stationary particle of mass m_2. Assuming a repulsive

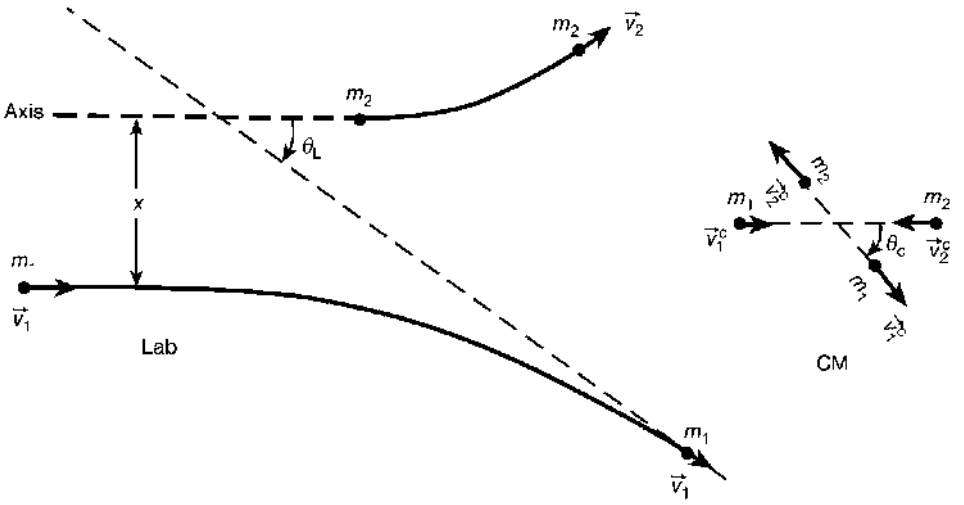

Figure 1.6. Particle trajectories in the laboratory and center of mass (prime indicates after collision)

electrostatic force (the final results are independent of the sign, although the trajectories are not) and defining the relative position vector

$$\boldsymbol{r} \equiv \boldsymbol{r}_1 - \boldsymbol{r}_2$$

and relative velocity vector

$$\boldsymbol{v} \equiv \boldsymbol{v}_1 - \boldsymbol{v}_2$$

the equations of motion can be combined to obtain

$$\frac{\mathrm{d}^2\boldsymbol{r}}{\mathrm{d}t^2} = \frac{m_1 + m_2}{m_1 m_2} \frac{e_1 e_2 \boldsymbol{r}}{4\pi\epsilon_0 |\boldsymbol{r}|^3} \equiv \frac{m_r^{-1} e_1 e_2 \boldsymbol{r}}{4\pi\epsilon_0 |\boldsymbol{r}|^3} \tag{1.23}$$

The solution of Eq. (1.23) is

$$\frac{1}{r} = \sqrt{1 + \frac{e_1^2 e_2^2}{x^2 \upsilon^4}} \cos(\theta_\mathrm{c} + \alpha) - \frac{e_1 e_2}{m_r \upsilon^2 x^2} \tag{1.24}$$

where θ_c is the scattering angle in the center-of-mass (CM) system, α is a constant, and x is the impact parameter defined in Fig. 1.6.

Working out the kinematics of an elastic collision (conservation of energy and momentum) yields an expression for the scattering angle in the CM system.

$$\tan\left(\frac{\theta_\mathrm{c}}{2}\right) = \frac{|e_1 e_2|}{m_r \upsilon^2 x 4\pi\epsilon_0} \tag{1.25}$$

and the relationship between the scattering angle in the lab and CM systems is determined by trigonometry

$$\cot\theta_\mathrm{L} = \left(\frac{m_1}{m_2}\right) \csc\theta_\mathrm{c} + \cot\theta_\mathrm{c} \tag{1.26}$$

Some special cases of Eq. (1.26) are of interest.

$$\begin{cases} m_1 \ll m_2\,, & \theta_{\mathrm{L}} \approx \theta_{\mathrm{c}} \\ m_1 = m_2\,, & \theta_{\mathrm{L}} = \frac{1}{2}\theta_{\mathrm{c}} \\ m_1 \gg m_2\,, & \theta_{\mathrm{L}} \approx \frac{m_2}{m_1}\sin\theta_{\mathrm{c}} \end{cases} \tag{1.27}$$

We have seen in Fig. 1.6 that the scattering event takes place in a plane. Actually, all particles of type 1 incident in the annular ring between x and $x + \mathrm{d}x$ from the axis will scatter into angles between θ_{c} and $\theta_{\mathrm{c}} + \mathrm{d}\theta_{\mathrm{c}}$ or, equivalently, between θ_{L} and $\theta_{\mathrm{L}} + \mathrm{d}\theta_{\mathrm{L}}$. For unit incident particle flux, the particle flux, $\mathrm{d}\sigma$, scattered into the differential solid angle $\mathrm{d}\Omega = 2\pi \sin\theta_{\mathrm{c}}\,\mathrm{d}\theta_{\mathrm{c}}$ is equal to the cross sectional area of the annulus between x and $x + \mathrm{d}x$

$$\mathrm{d}\sigma = \sigma(\theta_{\mathrm{c}})\,\mathrm{d}\Omega = \sigma(\theta_{\mathrm{c}})2\pi \sin\theta_{\mathrm{c}}\,\mathrm{d}\theta_{\mathrm{c}} = 2\pi x\,\mathrm{d}x \tag{1.28}$$

where $\sigma(\theta_{\mathrm{c}})$ is the Rutherford scattering cross section found by using Eq. (1.25)

$$\sigma(\theta_{\mathrm{c}}) \equiv \frac{2\pi x\,\mathrm{d}x}{2\pi \sin\theta_{\mathrm{c}}\,\mathrm{d}\theta_{\mathrm{c}}} = \frac{(e_1 e_2)^2}{\left(8\pi\epsilon_0 m_r \upsilon^2 \sin^2\frac{\theta_{\mathrm{c}}}{2}\right)^2} \tag{1.29}$$

Now, we will use these results to investigate the deflection of particles by Coulomb collisions. In particular, it will be shown that deflection through large angles (e.g., 90°) is much more probable as the result of multiple small-angle deflections than as the result of a single large-angle collision. This result has important consequences for our subsequent treatment of collision phenomena in plasmas.

First, consider the probability that a single interaction will scatter a particle through an angle $\gtrsim 90°$ in the CM system. Since the angle of scatter increases as the impact parameter, x, decreases, this probability is just equal to the area of the cylinder surrounding the axis with radius corresponding to the impact parameter which results in $\theta_{\mathrm{c}} = 90°$

$$\sigma(\theta_{\mathrm{c}} \geq 90°) = \pi x_{90}^2$$

The $\theta_{\mathrm{c}} = 90°$ impact parameter can be determined from Eq. (1.25), so that

$$\sigma(\theta_{\mathrm{c}} \geq 90°) = \frac{(e_1 e_2)^2}{\pi(4\epsilon_0 m_r \upsilon^2)^2} \tag{1.30}$$

Now, consider a series of small-angle collisions. In the limit $\theta_{\mathrm{c}} \to 0$, Eq. (1.25) yields an expression for the small-angle deflection in the CM system due to a single interaction

$$\Delta\theta_{\mathrm{c}} = \frac{2|e_1 e_2|}{4\pi\epsilon_0 m_r \upsilon^2 x} \tag{1.31}$$

The mean square deflection of a "test" particle that travels a distance L in a plasma with scattering center density n_2 is

$$\begin{aligned}\overline{(\Delta\theta_c)^2} &= n_2 L \int_{\Delta\theta_{\min}}^{\Delta\theta_{\max}} (\Delta\theta_c)^2 \sigma(\Delta\theta_c) 2\pi \sin(\Delta\theta_c)\, \mathrm{d}(\Delta\theta_c) \\ &= n_2 L \int_{x_{\min}}^{x_{\max}} (\Delta\theta_c)^2 2\pi x\, \mathrm{d}x \\ &= \frac{n_2 L}{2\pi} \left(\frac{e_1 e_2}{\epsilon_0 m_r \upsilon^2}\right)^2 \int_{x_{\min}}^{x_{\max}} \frac{\mathrm{d}x}{x} \\ &= \frac{n_2 L}{2\pi} \left(\frac{e_1 e_2}{\epsilon_0 m_r \upsilon^2}\right)^2 \ln\left(\frac{x_{\max}}{x_{\min}}\right)\end{aligned} \tag{1.32}$$

The limits ($\Delta\theta_{\max} \to x_{\min}, \Delta\theta_{\min} \to x_{\max}$) are related by Eq. (1.31). Since only encounters at distances of the order of the Debye length are treated as collisions because of the screened Coulomb potential, we can choose

$$x_{\max} = \lambda_2 = \left(\frac{\epsilon_0 T_2}{n_2 e_2^2}\right)^{\frac{1}{2}} \tag{1.33}$$

For the minimum impact parameter, we take x_{90}, the value leading to 90° collisions, which is certainly an upper limit on scattering angles for "small" deflections:

$$x_{\min} = \frac{|e_1 e_2|}{4\pi\epsilon_0 m_r \upsilon^2} \tag{1.34}$$

With these limits, Eq. (1.32) becomes

$$\overline{(\Delta\theta_c)^2} = n_2 L \left(\frac{e_1 e_2}{\epsilon_0 m_r \upsilon^2}\right)^2 \ln\, \Lambda \tag{1.35}$$

where the *Coulomb logarithm* is defined by

$$\ln\, \Lambda \equiv \ln\left(\frac{x_{\max}}{x_{\min}}\right) = \ln\left[12\pi \left(\frac{(\epsilon_0 T)^3}{n_2 e_2^4 e_1^2}\right)^{\frac{1}{2}}\right] \tag{1.36}$$

and the assumption $m_r \upsilon^2 \approx 3T$ has been used.

The mean free path for 90° deflection by small-angle scattering ($L = \lambda_{90}$) can be estimated from Eq. (1.35) by setting $\overline{(\Delta\theta_c)^2} = 1$. The corresponding cross section, σ_{90}, can then be constructed

$$\sigma_{90} \equiv \frac{1}{n_2 \lambda_{90}} = \frac{(e_1 e_2)^2 \ln\, \Lambda}{2\pi(\epsilon_0 m_r \upsilon^2)^2} \tag{1.37}$$

Finally, the relative probabilities for a particle undergoing a 90° deflection due to multiple small-angle collisions and due to a single large-angle collision can be found from

Eqs. (1.37) and (1.30):

$$\frac{\sigma_{90}}{\sigma(\theta_c > 90)} = 8 \ln \Lambda \tag{1.38}$$

The Coulomb logarithm is ~ 15 to 20 for thermonuclear plasmas. Thus, deflection through large angles via multiple small-angle collisions is about two orders of magnitude more probable than deflection via a single large-angle collision.

The characteristic time required for a 90° deflection in the CM system by multiple small-angle collisions is

$$\tau_{90} \equiv \frac{\lambda_{90}}{\upsilon} = \frac{2\pi\epsilon_0^2 m_r^2 \upsilon^3}{n_2(e_1e_2)^2 \ln \Lambda} = \frac{2\pi\sqrt{m_r}\epsilon_0^2(3T)^{\frac{3}{2}}}{n_2(e_1e_2)^2 \ln \Lambda} \tag{1.39}$$

For like-particle scattering (e.g., ions on ions or electrons on electrons), $m_r = m_2$ and

$$\left.\begin{matrix}\tau_{90}^{\mathrm{ii}} \\ \tau_{90}^{\mathrm{ee}}\end{matrix}\right\} = \frac{6\pi\sqrt{3}\sqrt{m_r}\epsilon_0^2(T)^{\frac{3}{2}}}{ne^4 \ln \Lambda} \tag{1.40}$$

where $m = \left.\begin{matrix} m_{\mathrm{i}} \\ m_{\mathrm{e}}\end{matrix}\right\}$ and $e^4 \to z^4e^4$ for τ_{90}^{ii}.

For electrons on ions

$$\tau_{90}^{ei} = \frac{6\sqrt{6\pi}\sqrt{m_{\mathrm{e}}}\epsilon_0^2(T)^{\frac{3}{2}}}{n_{\mathrm{i}}(ze^2)^2 \ln \Lambda} \tag{1.41}$$

and for ions on electrons the result is the same but with $n_{\mathrm{i}} \to n_{\mathrm{e}}$.

It follows from Eq. (1.27) that the deflection in the lab system is comparable to the deflection in the CM system when $m_1 \leq m_2$. Thus for like-particle scattering and for the scattering of electrons on ions the above expressions are also good estimates of the characteristic time for 90° deflection in the lab system.

However, for ions on electrons, $\Delta\theta_{\mathrm{L}} \sim m_{\mathrm{e}}/m_{\mathrm{i}}\Delta\theta_{\mathrm{c}}$. Thus the test particle must travel approximately $m_{\mathrm{i}}/m_{\mathrm{e}} \approx 2 \times 10^3$ times the distance (λ_{90}) required for a 90° deflection in the CM system before a 90° deflection occurs in the lab system. Consequently, the characteristic time for a 90° deflection in the lab is about $m_{\mathrm{i}}/m_{\mathrm{e}}$ times the characteristic time for a 90° deflection in the CM system. Thus

$$\tau_{90}^{ie} \approx \left(\frac{m_{\mathrm{i}}}{m_{\mathrm{e}}}\right)\tau_{90}^{ei} \tag{1.42}$$

From Eq. (1.39) we discover the ordering

$$\tau_{90}^{ee} \sim \tau_{90}^{ei} \sim \left(\frac{m_{\mathrm{e}}}{m_{\mathrm{i}}}\right)^{\frac{1}{2}}\tau_{90}^{ii} \sim \left(\frac{m_{\mathrm{e}}}{m_{\mathrm{i}}}\right)\tau_{90}^{ie} \tag{1.43}$$

In a typical thermonuclear plasma ($n \sim 10^{20}\,\mathrm{m}^{-3}$, $T = 10\,\mathrm{keV}$), $\tau_{90}^{ee} \sim \tau_{90}^{ei} \sim 10^{-4}\,\mathrm{s}$, $\tau_{90}^{ii} \sim 10^{-2}\,\mathrm{s}$, and $\tau_{90}^{ie} \sim 1\,\mathrm{s}$.

The energy transferred from particle 1 to particle 2 in a collision can be found from the collision kinematics (conservation of energy and momentum). For an initial energy of E_0, for particle l, the energy transferred, ΔE, is

$$\frac{\Delta E}{E_0} = \frac{4m_1 m_2}{(m_1 + m_2)^2} \sin^2 \frac{\theta_c}{2} \tag{1.44}$$

Multiple small-angle collisions that produce a 90° deflection in the CM system would cause an energy loss that can be estimated from Eq. (1.44) with $\theta_c = 90°$:

$$\frac{\Delta E}{E_0} \approx \frac{2m_1 m_2}{(m_1 + m_2)^2} \tag{1.45}$$

Thus like-particle collisions result in the transfer of about half of the initial energy in a 90° deflection time. For electrons scattering on ions or ions scattering on electrons, the fractional energy transfer in a 90° deflection is only about m_e/m_i. Hence the characteristic time for energy transfer, τ_e, is related to the 90° deflection time as

$$\begin{aligned}
\tau_E^{ee} &\sim \tau_{90}^{ee} \sim \tau_{90}^{ei} \\
\tau_E^{ii} &\sim \tau_{90}^{ii} \sim \left(\frac{m_i}{m_e}\right)^{\frac{1}{2}} \tau_{90}^{ei} \\
\tau_E^{ei} &\sim \frac{m_i}{m_e} \tau_{90}^{ei} \\
\tau_E^{ie} &\sim \frac{m_i}{m_e} \tau_{90}^{ei}
\end{aligned} \tag{1.46}$$

A number of important conclusions follow immediately from Eq. (1.46). The electrons in a thermonuclear plasma exchange energy with each other and reach an equilibrium distribution – equilibrate – on a very short time scale, about 10^{-4} s. The ions equilibrate with themselves on a time scale that is longer by a factor of ~ 40. The electrons transfer energy to ions, or vice versa, on a time scale that is $m_i/m_e \approx 2 \times 10^3$ times longer than the time scale required for the electrons to equilibrate with themselves.

Collisions have a randomizing effect on particle motion in a plasma. Consider the case of electrons drifting under the influence of an external electric field. Collisions tend to disorder the directed drift motion, which otherwise would be in the field direction. The equation of motion is

$$m_e \frac{dv_e}{dt} = -eE - \frac{m_e v_e}{\tau_{90}^{ei}} = -eE - \frac{e^4 n_e \ln \Lambda}{2\pi\epsilon_0^2 m_e v_e^2} \tag{1.47}$$

where the last term describes the rate of dissipation of ordered momentum due to collisions.

The first term on the right accelerates electrons (in the minus-direction for a positive E) and the second term acts to oppose the acceleration. Since the second term decreases with increasing v_e, electrons with velocity greater than the *Dreicer velocity*

$$\boldsymbol{v}_{eD} = \left(\frac{e^3 n_e \ln \Lambda}{2\pi m_e \epsilon_0^2 E}\right)^{\frac{1}{2}} \tag{1.48}$$

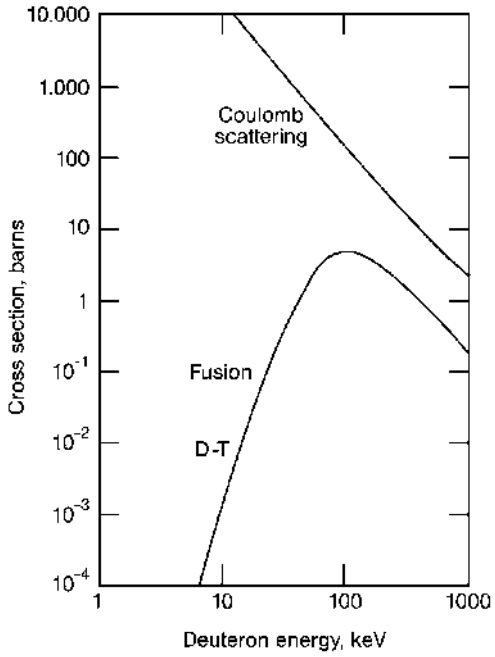

Figure 1.7. Fusion and Coulomb scattering cross sections (1 barn = 10^{-24} cm^2)

are accelerated indefinitely and become *runaway electrons*. When $n \approx 10^{20}\,\mathrm{m}^{-3}$ and $E = 10\,\mathrm{V}\cdot\mathrm{m}^{-1}$, electrons with energy greater than 5 keV are runaway electrons.

Defining the current density

$$j \equiv -e n_\mathrm{e} \upsilon_\mathrm{e} \tag{1.49}$$

and assuming that the drift velocity, υ_e, is much less than the random thermal velocity, υ_th, Eq. (1.47) becomes

$$\frac{m_\mathrm{e}}{e^2 n_\mathrm{e}} \frac{\mathrm{d}j}{\mathrm{d}t} = E - \eta j \tag{1.50}$$

where

$$\eta \equiv \frac{\sqrt{m_\mathrm{e}} z e^2 \ln \Lambda}{12\sqrt{3}\pi\epsilon_0^2 (T)^{\frac{3}{2}}} \tag{1.51}$$

is the plasma resistivity. Note that Eq. (1.50) is of the form of an Ohm's law for the plasma.

The cross sections for ion–ion Coulomb collisions and for fusion are plotted in Fig. 1.7. From this figure, we conclude that an ion will suffer a large number of collisions, on average, before it undergoes fusion. Thus, the effects of collisions on the plasma are quite important.

1.4 Electromagnetic Theory

Much of the theory of plasmas is concerned with electric and magnetic fields. Such fields arise from external sources and from net charge and current distributions in the plasma. Recall that the long-range interactions among the charged particles that constitute a plasma are treated collectively in terms of fields. In this section, we review the basic laws of electromagnetism and discuss some useful properties of fields.

Gauss' law states that the normal outward component of the electric displacement, $\boldsymbol{D}$, integrated over the surface bounding any volume is equal to the net charge contained within that volume

$$\int_{\mathrm{s}} \boldsymbol{D} \cdot \mathrm{d}\boldsymbol{s} = \int_{\upsilon} \rho \, \mathrm{d}^3 r \tag{1.52}$$

where ρ is the charge density. Using the divergence theorem on the LHS of Eq. (1.52) and requiring that the resulting equation be valid for arbitrary volumes leads to

$$\nabla \cdot \boldsymbol{D} = \rho \tag{1.53}$$

The magnetic field is divergence free – there is no magnetic equivalent of ρ. The normal outward component of the magnetic field, $\boldsymbol{B}$, integrated over any closed surface is zero:

$$\int_{\mathrm{s}} \boldsymbol{B} \cdot \mathrm{d}\boldsymbol{s} = 0 \tag{1.54}$$

Using the divergence theorem and the arbitrary volume argument leads to

$$\nabla \cdot \boldsymbol{B} = 0 \tag{1.55}$$

Since $\boldsymbol{B}$ is solenoidal (i.e., satisfies Eq. (1.55)), it follows that it can be derived from a vector potential function, $\boldsymbol{A}$:

$$\boldsymbol{B} = \nabla \times \boldsymbol{A} \tag{1.56}$$

Faraday's law states that a changing magnetic flux, Φ, produces an electromotive force around a closed loop

$$\oint \boldsymbol{E} \cdot \mathrm{d}\boldsymbol{l} = -\frac{\mathrm{d}}{\mathrm{d}t} \int_{\mathrm{s}} \boldsymbol{B} \cdot \mathrm{d}\boldsymbol{s} \equiv -\frac{\mathrm{d}}{\mathrm{d}t} \Phi \tag{1.57}$$

where s is any arbitrary surface bounded by the loop of arbitrary shape. If we assume that the loop and surface are fixed in time and make use of Stokes's theorem and the arbitrariness of the surface, Eq. (1.57) becomes

$$\nabla \times \boldsymbol{E} = -\frac{\partial \boldsymbol{B}}{\partial t} \tag{1.58}$$

Using Eq. (1.56) in Eq. (1.58) leads to

$$\nabla \times \left(E + \frac{\partial \boldsymbol{A}}{\partial t} \right) = 0 \tag{1.59}$$

from which we conclude that the quantity in brackets can be represented by the gradient of a scalar potential. Thus the electric field can be written

$$\boldsymbol{E} = -\nabla\phi - \frac{\partial \boldsymbol{A}}{\partial t} \equiv \boldsymbol{E}_\phi + \boldsymbol{E}_A \tag{1.60}$$

When the electric field is linearly related to the electric displacement by the permittivity $\epsilon_0 = 8.854 \times 10^{-12}\,\mathrm{F \cdot m^{-1}}$,

$$\boldsymbol{D} = \epsilon_0 \boldsymbol{E}_\phi \tag{1.61}$$

Eqs. (1.53) and (1.61) can be combined to obtain Poisson's equation for the electrostatic potential,

$$\nabla^2\phi = -\frac{\rho}{\epsilon_0} \tag{1.62}$$

The solution of Eq. (1.62) is

$$\phi(\boldsymbol{r}) = \frac{1}{4\pi\epsilon_0} \int \frac{\rho(\boldsymbol{r}')}{|\boldsymbol{r}' - \boldsymbol{r}'|}\, \mathrm{d}^3\boldsymbol{r}' \tag{1.63}$$

Thus the electrostatic contribution to the electric field can be determined from Eqs. (1.63) and (1.60), for a given charge distribution.

Ampere's law states that the normal component of the current plus the normal component of the time-rate-of-change of the electric displacement integrated over an arbitrary open surface produces a magnetomotive force around the closed loop bounding that surface:

$$\oint \boldsymbol{H} \cdot \mathrm{d}\boldsymbol{l} = \int_\mathrm{s} \boldsymbol{j} \cdot \mathrm{d}\boldsymbol{s} + \frac{\mathrm{d}}{\mathrm{d}t} \int_\mathrm{s} \boldsymbol{D} \cdot \mathrm{d}\boldsymbol{s} \tag{1.64}$$

where $\boldsymbol{H}$ is the magnetic intensity and $\boldsymbol{j}$ is the current density. Using Stoke's theorem and the arbitrariness of the surface leads to

$$\nabla \times \boldsymbol{H} = \boldsymbol{j} + \frac{\partial \boldsymbol{D}}{\partial t} \tag{1.65}$$

for a fixed surface.

Equations (1.52), (1.54), (1.57) and (1.64) are based on experimental observation and are sometimes referred to as the integral form of Maxwell's equations. Equations (1.53), (1.55), (1.58) and (1.65) are the familiar, differential forms of Maxwell's equations for a stationary medium. (We will be interested later in the counterparts of Eqs. (1.58) and (1.65) in a moving medium.)

Now, reconsider the vector potential, $\boldsymbol{A}$. Assume that the magnetic field and the magnetic intensity are linearly related through the permeability, $\mu_0 = 1.257 \times 10^{-6}\,\mathrm{H \cdot m^{-1}}$,

$$\boldsymbol{B} = \mu_0 \boldsymbol{H} \tag{1.66}$$

Substitute Eq. (1.56) into Eq. (1.65) and use Eq. (1.60) to obtain

$$\nabla \times (\nabla \times \boldsymbol{A}) = \nabla(\nabla \cdot \boldsymbol{A}) - \nabla^2 \boldsymbol{A} = \mu_0 \boldsymbol{j} - \mu_0 \epsilon_0 \nabla \frac{\partial \phi}{\partial t} + \mu_0 \epsilon_0 \frac{\partial^2 \boldsymbol{A}}{\partial t^2} \tag{1.67}$$

Substitute Eq. (1.60) into Eq. (1.53) to obtain

$$\nabla^2 \phi + \nabla \cdot \frac{\partial \boldsymbol{A}}{\partial t} = -\frac{\rho}{\epsilon_0} \tag{1.68}$$

Note that $\boldsymbol{A}$ is determined by Eq. (1.56) only within an arbitrary additive gradient of a scalar function, $R(\nabla \times \nabla R \equiv 0)$. It is convenient to choose the scalar function, R, so that

$$\nabla \cdot \boldsymbol{A} + \epsilon_0 \mu_0 \frac{\partial \phi}{\partial t} = 0 \tag{1.69}$$

Equation (1.69) is known as the *gauge condition* on the vector potential. This choice of gauge condition reduces Eq. (1.68) to

$$\nabla^2 \phi - \epsilon_0 \mu_0 \frac{\partial^2 \phi}{\partial t^2} = -\frac{\rho}{\epsilon_0} \tag{1.70}$$

and reduces Eq. (1.67) to

$$\nabla^2 \boldsymbol{A} - \epsilon_0 \mu_0 \frac{\partial^2 \boldsymbol{A}}{\partial t^2} = -\mu_0 \boldsymbol{j} \tag{1.71}$$

The solution to the time-independent version of Eq. (1.71) is

$$\boldsymbol{A}(\boldsymbol{r}) = \frac{\mu_0}{4\pi} \int \frac{\boldsymbol{j}(\boldsymbol{r}')}{|\boldsymbol{r} - \boldsymbol{r}'|} \, \mathrm{d}^3 \boldsymbol{r}' \tag{1.72}$$

The vector potential can be computed from the current distribution, in direct analogy with a computation of the scalar potential from the charge distribution according to Eq. (1.63). Knowing the scalar and vector potentials, one can compute the electrostatic and magnetic fields from Eq. (1.60) and Eq. (1.56), respectively. Thus electromagnetic theory provides the means for representing the collective, long-range interactions among the particles in a plasma in terms of fields.

The linear relationships of Eqs. (1.61) and (1.66) are only valid for an isotropic medium. More general constitutive relationships are frequently needed for plasmas, in which the magnetic field defines a unique set of directions in terms of which many phenomena are not isotropic. In general,

$$D_\alpha = \sum_\beta \epsilon_{\alpha\beta} E_\beta \quad \text{and} \quad B_\alpha = \sum_\beta \mu_{\alpha\beta} H_\beta \tag{1.73}$$

where α and β refer to the cartesian coordinates.

The concepts of electromagnetic energy density and electromagnetic stress associated with the fields follow directly from the manipulation of Eq. (1.73). Dotting $\boldsymbol{H}$ into Eq. (1.58) and $\boldsymbol{E}$ into Eq. (1.65), subtracting, and using the vector identity

$$\boldsymbol{H} \cdot \nabla \times \boldsymbol{E} - \boldsymbol{E} \cdot \nabla \times \boldsymbol{H} = \nabla \cdot (\boldsymbol{E} \times \boldsymbol{H})$$

leads to

$$\nabla \cdot (\boldsymbol{E} \times \boldsymbol{H}) + \frac{\partial}{\partial t}\left(\frac{\boldsymbol{E} \cdot \boldsymbol{D}}{2} + \frac{\boldsymbol{H} \cdot \boldsymbol{B}}{2}\right) + \boldsymbol{E} \cdot \boldsymbol{j} = 0 \tag{1.74}$$

Integrating Eq. (1.74) over an arbitrary volume and using the divergence theorem to convert the first term into a surface integral of the normal outward component of $\boldsymbol{S} = \boldsymbol{E} \times \boldsymbol{H}$ (the *Poynting vector*) over the closed surface bounding the volume leads to

$$\int_{\mathrm{s}} (\boldsymbol{E} \times \boldsymbol{H}) \cdot \mathrm{d}\boldsymbol{s} + \frac{\partial}{\partial t} \int \left(\frac{\boldsymbol{E} \cdot \boldsymbol{D}}{2} + \frac{\boldsymbol{H} \cdot \boldsymbol{B}}{2}\right) \mathrm{d}^3 r + \int \boldsymbol{E} \cdot \boldsymbol{j}\, \mathrm{d}^3 r = 0 \tag{1.75}$$

The first term represents the rate at which electromagnetic energy escapes across the surface. The first part of the integrand of the second term is the electrostatic energy density, which is equal to the work done to arrange the charges to create the electrostatic field. The second part of the integrand is the magnetic energy density, which is equal to the work done to establish the currents that create the magnetic field. The final term is the resistive work done by the electrostatic field on the charges within the volume.

Taking the cross product of Eq. (1.65) $\times \boldsymbol{D}$ and Eq. (1.58) $\times \boldsymbol{B}$, subtracting, and using Eqs. (1.53) and (1.55) yields

$$\rho \boldsymbol{E} + \boldsymbol{j} \times \boldsymbol{B} = \sum_{\alpha} \hat{\boldsymbol{n}}_{\alpha} \sum_{\beta} \frac{\partial T_{\alpha\beta}}{\partial x_{\beta}} - \epsilon_0 \mu_0 \frac{\partial \boldsymbol{S}}{\partial t} \tag{1.76}$$

The quantities $T_{\alpha\beta}$ are the components of the electromagnetic stress tensor, and $\hat{\boldsymbol{n}}_{\alpha}$ is the unit vector. In xyz coordinates

$$\begin{aligned}
T_{xx} &= E_x D_x + B_x H_x - \tfrac{1}{2}(\boldsymbol{E} \cdot \boldsymbol{D} + \boldsymbol{B} \cdot \boldsymbol{H}) \\
T_{xy} &= E_x D_y + B_x H_y \\
T_{xz} &= E_x D_z + B_x H_z \\
T_{yx} &= E_y D_x + B_y H_x \\
T_{yy} &= E_y D_y + B_y H_y - \tfrac{1}{2}(\boldsymbol{E} \cdot \boldsymbol{D} + \boldsymbol{B} \cdot \boldsymbol{H}) \\
T_{yz} &= E_y D_z + B_y H_z \\
T_{zx} &= E_z D_x + B_z H_x \\
T_{zy} &= E_z D_y + B_z H_y \\
T_{zz} &= E_z D_z + B_z H_z - \tfrac{1}{2}(\boldsymbol{E} \cdot \boldsymbol{D} + \boldsymbol{B} \cdot \boldsymbol{H})
\end{aligned} \tag{1.77}$$

Integrating Eq. (1.76) over an arbitrary volume and using the divergence theorem on the stress tensor term leads to

$$\int (\rho \boldsymbol{E} + \boldsymbol{j} \times \boldsymbol{B})\, \mathrm{d}^3 r = \sum_{\alpha} \hat{\boldsymbol{n}}_{\alpha} \sum_{\beta} \int T_{\alpha\beta}\, \mathrm{d}s_{\beta} - \int \epsilon_0 \mu_0 \frac{\partial \boldsymbol{S}}{\partial t}\, \mathrm{d}^3 r \tag{1.78}$$

The first term in Eq. (1.78) represents the force exerted on the charge and currents within the volume by the electrostatic and magnetic fields, respectively. The second term represents the stresses integrated over the surface bounding the volume. The final term represents the change in momentum density within the volume.

As a special example, consider the case in which $\boldsymbol{E} = 0$ and $\boldsymbol{B}$ is aligned along the z-axis. Then all the "off-diagonal" elements of the stress tensor vanish and

$$T_{xx} = T_{yy} = -T_{zz} = -\frac{B^2}{2\mu_0} \tag{1.79}$$

Thus $B^2/(2\mu_0)$ is the magnetic pressure in this case. We will make use of this subsequently when we consider the balancing of magnetic and kinetic pressures to establish a plasma equilibrium.

Problems for Chapter 1

1. Calculate the energy release in the fusion of 1 g of deuterium.
2. Calculate the deuterium and electron Debye lengths in a plasma with $T = 10\,\text{keV}$ and $n_\text{D} = n_\text{e} = 5 \times 10^{19}\,\text{m}^{-3}$.
3. Calculate the number of plasma ions and electrons within a sphere of radius the Debye length for problem 2.
4. Calculate and plot the electrostatic potential due to a single deuteron located at $r = 0$ for the plasma of problems 2 and 3.
5. Calculate the Coulomb repulsive force between two deuterons that are separated by two nuclear radii.
6. Calculate the deuteron and electron plasma frequencies for the plasma of problem 2.
7. Calculate the Rutherford scattering cross section between deuterons and electrons for scattering events of 1°, 10° and 90° in the CM system for the plasma of problem 2.
8. Calculate the 90° multiple collision deflection times for ions and electrons scattering with ions and electrons for the plasma of problem 2.
9. Calculate the characteristic energy transfer times for a deuterium ion to other deuterium ions and to electrons for the plasma of problem 2.
10. Calculate the Dreicer runaway electron velocity for the plasma of problem 2 in electric fields of $1\,\text{V}\cdot\text{m}^{-1}$, $5\,\text{V}\cdot\text{m}^{-1}$ and $10\,\text{V}\cdot\text{m}^{-1}$.
11. Calculate the plasma resistivity for the plasma of problem 2.

12. Calculate the kinetic pressure of the plasma of problem 2.
13. Calculate the magnetic pressure of fields of $B = 1\,\mathrm{T}$ and $10\,\mathrm{T}$.
14. Calculate the mass of deuterium and tritium that will be consumed daily in a fusion power plant producing 3000 MWth fusion power.